Topological Pumping of Photons in Nonlinear Resonator Arrays

Jirawat Tangpanitanon,[1,*] Victor M. Bastidas,[1] Sarah Al-Assam,[2] Pedram Roushan,[3]
Dieter Jaksch,[2,1] and Dimitris G. Angelakis[1,4,†]
[1]Centre for Quantum Technologies, National University of Singapore, 3 Science Drive 2, Singapore 117543, Singapore
[2]Clarendon Laboratory, University of Oxford, Parks Road, Oxford OX1 3PU, United Kingdom
[3]Google Inc., Santa Barbara, California 93117, USA
[4]School of Electrical and Computer Engineering, Technical University of Crete, Chania, Crete 73100, Greece
(Received 15 July 2016; published 17 November 2016)

We show how to implement topological or Thouless pumping of interacting photons in one-dimensional nonlinear resonator arrays by simply modulating the frequency of the resonators periodically in space and time. The interplay between the interactions and the adiabatic modulations enables robust transport of Fock states with few photons per site. We analyze the transport mechanism via an effective analytic model and study its topological properties and its protection to noise. We conclude by a detailed study of an implementation with existing circuit-QED architectures.

DOI: 10.1103/PhysRevLett.117.213603

Introduction.—In the third century B.C., Archimedes figured out how to pump water up a hill using a rotating screw simply by exploiting the laws of classical physics. Two millennia later, Thouless proposed topological pumping for the robust transport of quantum particles in 1D periodic lattices by means of an analogous adiabatic and cyclic deformation of the underlying Hamiltonian [1]. In addition, he showed that the number of particles transported during one pump cycle is quantized and can be related to a topological invariant known as the Chern number [2]. As a consequence, the transport is robust against small disorder and perturbation [3–8].

Recently, there have been experimental demonstrations of such topological or "Thouless" pumping for noninteracting particles using optical lattices [9,10] and waveguide arrays [11,12]. Topological pumping in the case of interacting systems remains relatively unexplored. Previous works have theoretically explored related adiabatic quantum pumping in quantum wires [13], quantum dots [14–16], and electrons in a mesoscopic conductor [17]. However, the latter schemes do not involve a lattice structure, which is essential for achieving topological protection. In the case of interacting systems in a 1D lattice, topological pumping has been explored formally in the bosonic Bose-Hubbard model with correlated hopping and nearest-neighbor repulsion [18,19], and in interacting spin systems [20].

In this Letter, we propose topological pumping of interacting particles for the reliable transport of bosonic Fock states in 1D lattices. This is qualitatively different from the standard Thouless pumping which does not allow transporting Fock states [3–12]. We study the robustness of the transport against disorder for a range of parameters. In addition, the mechanism we propose here can be realized in a variety of quantum technology platforms such as ultracold quantum gases [21], trapped ions [22], and interacting photons in circuit QED [23–28]. Because of extended usage of photonic Fock states in quantum information processing [29], we demonstrate our proposal in the context of nonlinear resonator arrays [30–33] and conclude with a detailed study of a circuit-QED setup implementing our proposal.

The system.—We consider a nonlinear resonator array of size L implemented in circuit QED as discussed in Ref. [34]. The array is described by the Bose-Hubbard model with attractive interactions and spatially modulated on-site energies

$$H(t) = \sum_{m=0}^{L-1} \omega_m(t)\hat{n}_m - J\sum_{m=0}^{L-2}(\hat{a}_m^\dagger \hat{a}_{m+1} + \text{H.c.}) + \frac{U}{2}\sum_{m=0}^{L-1}\hat{n}_m(\hat{n}_m - 1), \tag{1}$$

where $\hat{n}_m = \hat{a}_m^\dagger \hat{a}_m$ and $\hat{a}_m^\dagger$, $\hat{a}_m$ are bosonic creation and annihilation operators, respectively [34]. In addition, $\omega_m(t) = \omega_0 + \Delta\cos[2\pi m/3 + \phi(t)]$ is the frequency of the resonator, $\Delta > 0$ is a modulation amplitude, $\phi(t)$ is a time-dependent modulation phase, $U < 0$ is an attractive Kerr nonlinearity, and $J > 0$ is the hopping strength. Since the number of photons is conserved, the first term $\sum_{m=1}^{L-1}\omega_0\hat{n}_m$ can be eliminated from Eq. (1). The modulation phase is adiabatically swept in time as $\phi(t) = \Omega t + \phi_0$, where Ω is the ramping speed, and ϕ_0 is an initial modulation phase. This sweeping is possible in circuit QED, as the frequency of the resonator can be tuned on the fly using a flux bias [25,27]. For simplicity, we choose L to be an integer multiple of 3. Hence, the array can be thought of as an array of trimers of size $L/3$ as it is depicted in Fig. 1(a). For convenience, we introduce the index $l \in \{0, \ldots, L/3 - 1\}$ to label the trimers. Since the

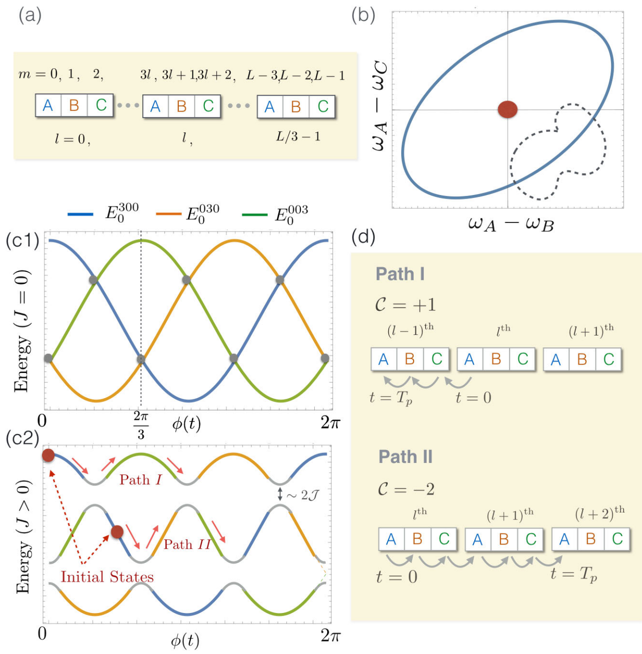

FIG. 1. (a) Depictions of the sublattices A, B, and C at the sites $3l$, $3l+1$, and $3l+2$, respectively. (b) Pump cycle in the 2D parameter space spanned by $(\omega_A - \omega_B)$ and $(\omega_A - \omega_C)$ for $U = -J$. It encircles the critical point at $\omega_A = \omega_B = \omega_C$ labeled as a red dot. A gray-dashed path is displayed as an example of a topologically trivial path. (c1) On-site energies $E_0^\mu(t) = \langle\mu|H_0^l(t)|\mu\rangle_l$ as a function of the modulation phase $\phi(t)$. Different bands $\mu = 300$, 030, 003 are labeled as blue, green, and orange, respectively. Crossing points between two bands are labeled as gray dots. (c2) Eigenenergies emerging in the presence of a small photon hopping $J \ll \Delta$. As discussed in the text, near every crossing point in (c1), an effective three-photon hopping can be derived, which converts these points into the anticrossing points shown in (c2) with the gap $2\mathcal{J} = \sqrt{2}J^3/U^2$. As a result, the quantized transport of the Fock states can then be understood by adiabatically following one of the bands in (c2). (d) Illustration of the quantized transport. $T_p = 2\pi/\Omega$ is the pumping period. In the path I, the state $|300\rangle_l$ is initialized at the highest band with $\phi(0) = 0$. The three photons hop from one site to another when passing through each anticrossing point. Since in the upper band there are three anticrossing points for $\forall\phi(t) \in [0, 2\pi)$, after one pump cycle, the three photons are pumped from $|300\rangle_l$ to $|300\rangle_{l-1}$. The transport corresponds to the effective Chern number $\mathcal{C} = 1$. For path II, the transport has different topology with $\mathcal{C} = -2$. The lowest band has the same topology as the highest one.

modulation wavelength is also 3, the Hamiltonian that acts on each trimer is identical. Later in the text, we will refer to the three sublattices at positions $3l$, $3l+1$, and $3l+2$ within the lth trimer as A, B, and C, respectively [see Fig. 1(a)].

Our pumping protocol is shown in Fig. 1(b). It corresponds to a loop in a 2D parameter space with $U = -J$. Our two varying parameters are the frequency differences $\omega_A - \omega_B$ and $\omega_A - \omega_C$ between two resonators in a trimer, where $\omega_A = \omega_0 + \Delta\cos[\phi(t)]$, $\omega_B = \omega_0 + \Delta\cos[\phi(t) + 2\pi/3]$, and $\omega_C = \omega_0 + \Delta\cos[\phi(t) + 4\pi/3]$. In Ref. [39], we show that for $U = -J$ this loop encloses the critical point when $\omega_A = \omega_B = \omega_C$. We will later show that the spectrum along this loop is gapped. As a result, the topology of the pump is said to be invariant under deformation of this loop as long as it encloses the critical point [2].

Topological transport of Fock states.—Let us begin by considering three-photon Fock states within a given trimer, i.e., $|300\rangle_l$, $|030\rangle_l$, and $|003\rangle_l$. In the following, we will show that at the right regime, an effective three-photon hopping can be derived, allowing the three-photon Fock states to be efficiently transported through the array.

To illustrate the above, let us decompose the Hamiltonian as $H(t) = \sum_l H_0^l(t) + \lambda V$, where $H_0^l(t) = \sum_{m=3l}^{3l+2} [\Delta\cos[2\pi m/3 + \phi(t)]\hat{n}_m + (U/2)\hat{n}_m(\hat{n}_m - 1)]$ and $\lambda V = -J\sum_m(\hat{a}_m^\dagger \hat{a}_{m+1} + \mathrm{H.c.})$. In the case $J = 0$, we define the on-site energies of the three-photon Fock states as $E_0^\mu(t) = \langle\mu|H_0^l(t)|\mu\rangle_l$ for $\mu \in \{300, 030, 003\}$. Note that the energies $E_0^\mu(t)$ do not depend on the trimer index l. The energies $E_0^\mu(t)$ are depicted in Fig. 1(c1) as a function of $\phi(t)$. When including a small but nonvanishing hopping strength $J \ll \Delta$, the crossings in Fig. 1(c1) become anticrossings, as shown in Fig. 1(c2). This is due to an effective three-photon hopping between two neighboring sites that happens near an anticrossing (we outline the mechanism below). As a result, the energy spectrum when $0 < J \ll \Delta$ is separated into three gapped bands for $\forall\phi(t) \in [0, 2\pi)$, as depicted in Fig. 1(c2). The quantized transport of the three photons can then be understood simply by adiabatically following one of these bands [see Figs. 1(c2)and 1(d)].

To obtain the above picture, we derive the effective three-photon hopping by first identifying relevant states near a given anticrossing point. To do this, let us consider a particular crossing point in Fig. 1(c1) when $J = 0$, for example, at $\phi(t^*) = 2\pi/3$. There, the two crossing bands $E_0^{300}(t^*) = E_0^{030}(t^*)$ are far separated from the third one, $E_0^{003}(t^*)$. Hence, when including a small hopping $J \ll \Delta$, the relevant three-photon states in the lth trimer are $|300\rangle_l$, $|030\rangle_l$, $|210\rangle_l$, and $|120\rangle_l$. We then note that when $J = 0$, the states $|300\rangle_l$ and $|030\rangle_l$ have the same on-site energies, $\epsilon_3 = E_0^{300}(t^*) = E_0^{030}(t^*) = -3\Delta/2 + 3U$ and so do the states $|210\rangle_l$ and $|120\rangle_l$ with the on-site energy $\epsilon_2 = -3\Delta/2 + U$. Since $\epsilon_2 - \epsilon_3 = -2U$, in the limit $0 < \sqrt{3}J < -2U$, one can do adiabatic elimination of the intermediate states $|210\rangle_l$ and $|120\rangle_l$, during the process $|300\rangle_l \to |210\rangle_l \to |120\rangle_l \to |030\rangle_l$. This is done by expanding the Hamiltonian $H(t^*)$ in $\sqrt{3}J/2U$ up to the third order using the Schreffer-Wolff transformation [52]. As a result, an effective three-photon hopping process can be derived as $\tilde{H}_J^l(t^*) = -\mathcal{J}(|300\rangle_l\langle 030|_l + |030\rangle_l\langle 300|_l)$, where $\mathcal{J} = J^3/\sqrt{2}U^2$ [39]. Similar analysis can be applied for all anticrossing points in Fig. 1(c2). We stress here that

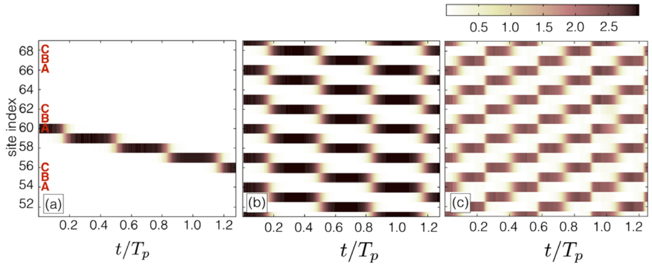

FIG. 2. Density plot $\langle \hat{n}_m \rangle$ as a function of time, illustrating a quantized transport of a three-photon state. In (a) a three-photon Fock state $|3\rangle$ is prepared at the sublattice A located at the middle of an array of size $L = 120$ ($\Delta = 10J$, $\phi_0 = 0$, $U = -J$, $T_p = 2\pi/\Omega$, and $\Omega = 0.01J$). In (b) each sublattice A is filled with the three-photon Fock state. We left five trimers near the edges empty to avoid boundary effects during the evolution. The density plot shows a clear steplike behavior in both cases. In (c) the initial modulation phase is set at $\phi_0 = \pi/2$, and the ramping speed is $\Omega_p = 0.002J$. As discussed in the text, this results in a quantized transport in the reversed direction and twice the speed of the pump. In (b) and (c) the local Hilbert space in the numerics is truncated at the five-photon Fock state.

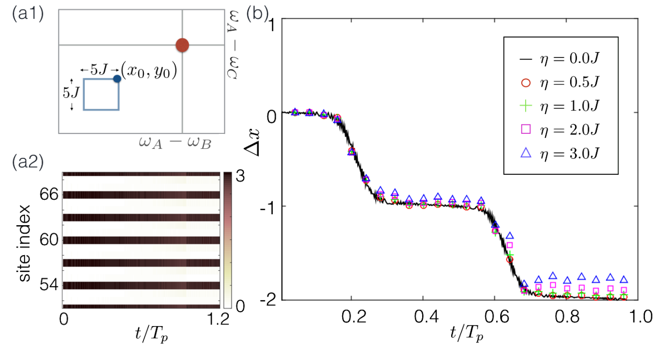

FIG. 3. (a1) Illustration of a topologically trivial pumping scheme in the 2D parameter space. We fix $\omega_A = \omega_0$ and vary ω_B and ω_C as a square loop with the starting point $(x_0, y_0) = [-\Delta\cos(2\pi/3), -\Delta\cos(4\pi/3)]$. The pumping period T_p and the initial state are the same as those in Fig. 2(b). (a2) Density plot showing the corresponding motion. (b) C.m. displacement, Δx, of a three-photon state as a function of time with the nontrivial pumping topology in the presence of random noise. A black solid line corresponds to the perfect case with no noise $\eta = 0$. The parameters of the Hamiltonian and the initial state are the same as those in Fig. 2(a). The plot shows that the quantized motion is robust against weak perturbations, such that the amplitude of the noise η is smaller than the smallest energy gap $2\mathcal{J}$.

this perturbation does not work in the absence of interactions, i.e., when $U = 0$.

The three gapped bands in Fig. 1(c2) resulting from the effective three-photon hopping are said to have different topologies due to their distinct transport properties. For example, as shown in Fig. 1(d), the states in the middle band move in the opposite direction with twice the speed as those in the upper band. We define the effective Chern number $\mathcal{C}$—a topologically invariant quantity for a given band—as the number of trimers that the three photons pass during one pump cycle, which is equivalent to the Wannier center displacement [2]. Hence, the states in the highest and the middle bands can be assigned with the Chern numbers $\mathcal{C} = +1$ and $\mathcal{C} = -2$, respectively. The sign indicates whether the direction of motion is the same (+) as or opposite (−) to that of the pump. [Recall that the modulation wave $\Delta\cos(2\pi m/3 + \Omega t + \phi_0)$ moves towards the leftmost site $m = 0$].

In Fig. 2(a), we numerically show the quantized transport by plotting the density $\langle \hat{n}_m \rangle$ as a function of time. The three-photon Fock state is initialized at the site $m = 60$ (sublattice A) of an array of size $L = 120$. Time evolution is performed using time-evolving block decimation [53,54] with parameters given in Ref. [39]. The parameters of the Hamiltonian are $\Delta = 10J$, $U = -J$, $\Omega = 0.01J$, and $\phi_0 = 0$. The density plot shows a clear steplike motion with $\mathcal{C} = 1$, as expected.

One can also imagine filling each trimer l with the same three-photon Fock states $|300\rangle_l$, i.e., the unit-filling condition [see Fig. 2(b)]. Because photons between neighboring trimers are always two sites apart, they are effectively decoupled from each other throughout the evolution. Hence, a similar quantized transport occurs for many-photon states.

The quantized transport with $\mathcal{C} = -2$ is shown in Fig. 2(c), where the initial modulation phase is changed to $\phi_0 = \pi/2$ while keeping the initial state the same as that in Fig. 2(b). The motion is reversed with twice the speed compared to the one in Fig. 2(b), as expected. To further emphasize the topological nature of the transport, in Fig. 3(a1) we also change our pumping scheme to the one that does not enclose the critical point in the 2D parameter space, while keeping the starting and the end points the same as before. As shown in Fig. 3(a2), photons following this path remain localized throughout the evolution, corresponding to a topologically trivial transport with $\mathcal{C} = 0$, as expected.

Robustness analysis.—The quantized transport discussed here so far is protected by the energy gap proportional to $2\mathcal{J}$. Hence, it is robust against small perturbations. To illustrate this, we add random noise to the system as $H_{\rm noise} = \eta \sum_m r_m(t)\hat{n}_m$, where η is the noise amplitude, and $r_m(t) \in [0, 1]$ is a random number drawn differently for each site at each time step. The parameters of the Hamiltonian and the initial state are the same as in Fig. 2(a). The center of mass (c.m.) of the three photons as a function of time with an increasing η is shown in Fig. 3. It can be seen that the quantized motion is robust against weak perturbations, $\eta \lesssim J$. As the noise amplitude η becomes comparable to the smallest energy gap, which in this case is $2\mathcal{J} \sim 1.4J$, the c.m. is biased towards the rightmost site ($m = L - 1$). This is expected, as random noise introduces coupling to states from other bands. As shown before, these

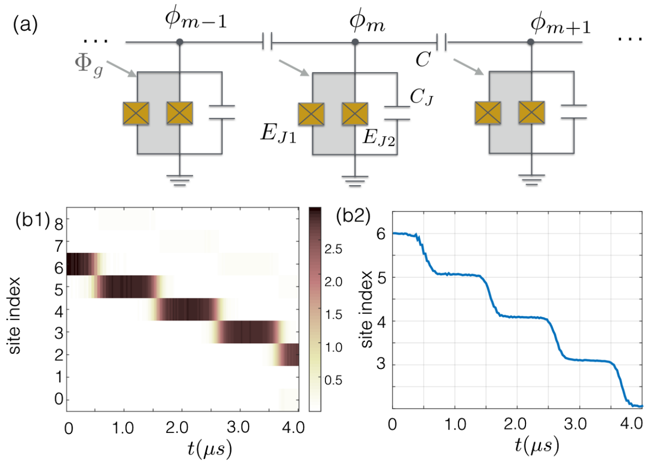

FIG. 4. (a) Circuit-QED diagram showing an implementation of the Hamiltonian $H(t)$. We introduce the flux variable, which is defined as $\phi_m = -\int V_m dt$, where V_m is a voltage at the corresponding position. As shown in Ref. [39], this quantity can be quantized to the form $\phi_m = \alpha(a_m + a_m^\dagger)$, where α is a constant depending on the circuit's elements. The Josephson junctions E_{J1}, E_{J2} and the shunting capacitor C_J act as a nonlinear resonator, whose frequency can be tuned via the flux bias Φ_g. Each resonator is coupled by the capacitor C. (b1), (b2) Quantum trajectory simulations of a nine-site lossy resonator array. (b1) Density plot $\langle \hat{n}_m \rangle$ as a function of time in a lossy case. (b2) Center of mass of the three photons as a function of time. A clear steplike behavior is observed in both plots.

states are transported in opposite directions. Therefore, when $\eta \gtrsim \mathcal{J}$, the c.m. deviates from the ideal case over time.

Circuit-QED implementation.—The localization due to attractive interaction and large modulation $\Delta \gg J$ in our system allow signatures of topological pumping to be visible with an existing finite-size array, as small as $L = 9$ as implemented in Ref. [26] [see Fig. 4(a) and, also, Ref. [39] for more details on the implementation]. To show this, we numerically solve the Lindblad master equation involving realistic photon loss, which is expressed as

$$\frac{\partial \rho}{\partial t} = -i[H(t), \rho] + \frac{1}{2T_1}\sum_m (2\hat{a}_m \rho \hat{a}_m^\dagger - \{\hat{n}_m, \rho\}), \quad (2)$$

where ρ is a density matrix, and $T_1 = 20\ \mu$s is a photon lifetime. We choose realistic parameters of the Hamiltonian as $\Delta = 0.4$ GHz, $\Omega = 2$ MHz, $J = 40$ MHz, and $U = -40$ MHz. A 5% disorder is added to U to mimic the fact that nonlinearities of Josephson junctions are different. Three photons are initialized at the site $m = 6$ with $\phi_0 = 0$. Time evolution is performed using the quantum trajectories [55] with parameters given in Ref. [39]. The density and the c.m. plots as a function of time are shown in Figs. 4(b1) and 4(b), respectively. A clear steplike motion is observed in both plots.

In conclusion, we have proposed a new mechanism of topological transport of interacting particles. The interactions enable robust transport of few-photon Fock states against disorder. We have also discussed in detail how to implement the above in existing circuit-QED architectures.

We note that our scheme here can be trivially generalized to Fock states other than three. For example, by initializing two photons per trimer and choosing appropriate U/J, Fock states with a $2/3$ filling can be transported. In addition, although we have been focusing on the transport of Fock states, entangled states are also created during the hopping process and can be transported through by adjusting the initial conditions. Hence, in the future it would be interesting to characterize this entanglement, which emerges between the two neighboring sites during population transfer, and seek applications in quantum information processing.

This research is supported by Singapore Ministry of Education Academic Research Fund Tier 3 (Grant No. MOE2012-T3-1-009), National Research Foundation (NRF) Singapore and the Ministry of Education, Singapore under the Research Centres of Excellence programme. The research leading to these results has received funding from the European Research Council under the European Union's Seventh Framework Programme (FP7/2007-2013) Grant Agreement No. 319286 Q-MAC and UK Engineering and Physical Sciences Research Council (EPSRC) funding EP/K038311/1.

*a0122902@u.nus.edu
†dimitris.angelakis@qubit.org

[1] D. J. Thouless, Phys. Rev. B **27**, 6083 (1983).
[2] J. K. Asbóth, L. Oroszlány, and A. Pályi, *A Short Course on Topological Insulators* (Springer International Publishing, New York, 2016), Vol. 919.
[3] Q. Niu and D. J. Thouless, J. Phys. A **17**, 2453 (1984).
[4] J. E. Avron and R. Seiler, Phys. Rev. Lett. **54**, 259 (1985).
[5] F. Mei, J.-B. You, D.-W. Zhang, X. C. Yang, R. Fazio, S.-L. Zhu, and L. C. Kwek, Phys. Rev. A **90**, 063638 (2014).
[6] P. Marra, R. Citro, and C. Ortix, Phys. Rev. B **91**, 125411 (2015).
[7] L. Zhou, D. Y. Tan, and J. Gong, Phys. Rev. B **92**, 245409 (2015).
[8] R. W. Bomantara, G. N. Raghava, L. Zhou, and J. Gong, Phys. Rev. E **93**, 022209 (2016).
[9] M. Lohse, C. Schweizer, O. Zilberberg, M. Aidelsburger, and I. Bloch, Nat. Phys. **12**, 350 (2016).
[10] S. Nakajima, T. Tomita, S. Taie, T. Ichinose, H. Ozawa, L. Wang, M. Troyer, and Y. Takahashi, Nat. Phys. **12**, 296 (2016).
[11] Y. E. Kraus, Y. Lahini, Z. Ringel, M. Verbin, and O. Zilberberg, Phys. Rev. Lett. **109**, 106402 (2012).
[12] M. Verbin, O. Zilberberg, Y. Lahini, Y. E. Kraus, and Y. Silberberg, Phys. Rev. B **91**, 064201 (2015).
[13] R. Citro, N. Andrei, and Q. Niu, Phys. Rev. B **68**, 165312 (2003).

[14] I. L. Aleiner and A. V. Andreev, Phys. Rev. Lett. **81**, 1286 (1998).
[15] J. Splettstoesser, M. Governale, J. König, and R. Fazio, Phys. Rev. Lett. **95**, 246803 (2005).
[16] D. Fioretto and A. Silva, Phys. Rev. Lett. **100**, 236803 (2008).
[17] E. Sela and Y. Oreg, Phys. Rev. Lett. **96**, 166802 (2006).
[18] E. Berg, M. Levin, and E. Altman, Phys. Rev. Lett. **106**, 110405 (2011).
[19] D. Rossini, M. Gibertini, V. Giovannetti, and R. Fazio, Phys. Rev. B **87**, 085131 (2013).
[20] D. Meidan, T. Micklitz, and P. W. Brouwer, Phys. Rev. B **84**, 075325 (2011).
[21] I. Bloch, J. Dalibard, and S. Nascimbene, Nat. Phys. **8**, 267 (2012).
[22] R. Blatt and C. F. Roos, Nat. Phys. **8**, 277 (2012).
[23] A. A. Houck, H. E. Türeci, and J. Koch, Nat. Phys. **8**, 292 (2012).
[24] M. H. Devoret and R. J. Schoelkopf, Science **339**, 1169 (2013).
[25] Y. Chen *et al.*, Phys. Rev. Lett. **113**, 220502 (2014).
[26] J. Kelly *et al.*, Nature (London) **519**, 66 (2015).
[27] J. Koch, T. M. Yu, J. Gambetta, A. A. Houck, D. I. Schuster, J. Majer, A. Blais, M. H. Devoret, S. M. Girvin, and R. J. Schoelkopf, Phys. Rev. A **76**, 042319 (2007).
[28] P. Macha, G. Oelsner, J.-M. Reiner, M. Marthaler, S. André, G. Schön, U. Hübner, H.-G. Meyer, E. Il'ichev, and A. V. Ustinov, Nat. Commun. **5**, 5146 EP (2014).
[29] P. Kok and B. W. Lovett, *Introduction to Optical Quantum Information Processing* (Cambridge University Press, Cambridge, England, 2010).
[30] C. Noh and D. G. Angelakis, arXiv:1604.04433.
[31] D. G. Angelakis, M. F. Santos, and S. Bose, Phys. Rev. A **76**, 031805 (2007).
[32] M. J. Hartmann, F. G. S. L. Brandao, and M. B. Plenio, Nat. Phys. **2**, 849 (2006).
[33] A. D. Greentree, C. Tahan, J. H. Cole, and L. C. L. Hollenberg, Nat. Phys. **2**, 856 (2006).
[34] In the semiclassical regime $\langle \hat{n}_m \rangle \gg 1$, the Hamiltonian in Eq. (1) is known as the nonlinear Harper model. Previous works have used the mean-field description to study the spreading of an initially localized wave packet [35–38]. In the absence of interactions $U = 0$, the model can be mapped to the 2D integer quantum Hall system. The latter has been realized in optical waveguide arrays [11].
[35] Y. Lahini, R. Pugatch, F. Pozzi, M. Sorel, R. Morandotti, N. Davidson, and Y. Silberberg, Phys. Rev. Lett. **103**, 013901 (2009).
[36] O. Manela, M. Segev, D. N. Christodoulides, and D. Kip, New J. Phys. **12**, 053017 (2010).
[37] Z. Zhang, P. Tong, J. Gong, and B. Li, Phys. Rev. E **83**, 056205 (2011).
[38] M. Larcher, T. V. Laptyeva, J. D. Bodyfelt, F. Dalfovo, M. Modugno, and S. Flach, New J. Phys. **14**, 103036 (2012).
[39] See Supplemental Material at http://link.aps.org/supplemental/10.1103/PhysRevLett.117.213603, which includes Refs. [40–51], for a detailed derivation of the effective three-photon hopping, a mean-field analysis of the critical point, and the circuit-QED implementation of the model.
[40] K. Bergmann, H. Theuer, and B. W. Shore, Rev. Mod. Phys. **70**, 1003 (1998).
[41] N. Lörch, J. Qian, A. Clerk, F. Marquardt, and K. Hammerer, Phys. Rev. X **4**, 011015 (2014).
[42] V. M. Bastidas, I. Omelchenko, A. Zakharova, E. Schöll, and T. Brandes, Chimera states in quantum mechanics, in *Control of Self-Organizing Nonlinear Systems*, edited by E. Schöll, S. H. L. Klapp, and P. Hövel (Springer, Berlin, Heidelberg, 2016), pp. 315–336.
[43] M. Leib, F. Deppe, A. Marx, R. Gross, and M. J. Hartmann, New J. Phys. **14**, 075024 (2012).
[44] J. Majer, J. M. Chow, J. M. Gambetta, J. Koch, B. R. Johnson, J. A. Schreier, L. Frunzio, D. I. Schuster, A. A. Houck, A. Wallraff, A. Blais, M. H. Devoret, S. M. Girvin, and R. J. Schoelkopf, Nature (London) **449**, 443 (2007).
[45] M. A. Sillanpaa, J. I. Park, and R. W. Simmonds, Nature (London) **449**, 438 (2007).
[46] P. Jung, A. V. Ustinov, and S. M. Anlage, Supercond. Sci. Technol. **27**, 073001 (2014).
[47] V. Pierro and G. Filatrella, Physica (Amsterdam) **517C**, 37 (2015).
[48] H. R. Mohebbi and A. H. Majedi, IEEE Trans. Appl. Supercond. **19**, 891 (2009).
[49] M. H. Devoret, in *Quantum Fluctuations (Les Houches Session LXIII)*, edited by S. Reynaud, E. Giacobino, and J. Zinn-Justin (Elsevier, New York, 1997), pp. 351–386.
[50] A. Nunnenkamp, J. Koch, and S. M. Girvin, New J. Phys. **13**, 095008 (2011).
[51] P. Roushan *et al.*, Nat. Phys. (2016), doi: 10.1038/nphys3930.
[52] C. Cohen-Tannoudji, J. Dupont-Roc, and G. Grynberg, *Atom-Photon Interaction: Basic Process and Application* (Wiley, New York, 1998).
[53] S. Al-Assam, S. Clark, D. Jaksch, and TNT Development Team, arXiv:1610.02244.
[54] G. Vidal, Phys. Rev. Lett. **91**, 147902 (2003).
[55] A. J. Daley, Adv. Phys. 63 (2014).
[56] R. Barends *et al.*, Nature (London) **508**, 500 (2014).
[57] F. Verstraete, V. Murg, and J. Cirac, Adv. Phys. **57**, 143 (2008).
[58] R. Ors, Ann. Phys. (Amsterdam) **349**, 117 (2014).
[59] U. Schollwck, Ann. Phys. (Amsterdam) **326**, 96 (2011).
[60] G. S. Ng and T. Kottos, Phys. Rev. B **75**, 205120 (2007).